

optical variability scale. One might therefore expect the M33 nucleus similarly to have an x-ray variability time shorter than the optical time scale by a factor of ~100, or roughly 10^2 - 10^3 sec. But no rapid (10^2 - $2 \cdot 10^4$ sec) x-ray variability has yet been detected (Refs. 1, 2) in M33.

Two groups of observers have measured the x-ray emission of M33 by means of the Einstein Observatory with different instruments but at practically the same time.^{1,2} The closest spacing between observations with the two instruments (the IPC, the HRI) was 3^d . Although the two counters differed in sensitivity and to some extent in their energy range (0.15-4.5, 0.1-3 keV, respectively), Markert and Rallis² have converted the HRI luminosity of the nucleus to the IPC acceptance band, enabling the two sets of observations to be intercompared. It turns out that in January 1980 the x-ray luminosity dropped almost to one-half in a 4^d interval.

These x-ray data were acquired in 1979-1980, the time when according to the estimate of Gallagher et al.⁴ the M33 nucleus was in its minimum state. If that is true, then at the present time, when the nucleus is 1^m brighter optically, there might well be a concomitant (2-3)-fold rise in the x-ray flux, conceivably accompanied by rapid variability. Thus it

would be highly worthwhile to continue making x-ray and optical observations.

- ¹K. S. Long, S. D'Odorico, P. A. Charles, and M. A. Dopita, *Astrophys. J.* **246**, L61 (1981).
- ²T. H. Markert and A. D. Rallis, *Astrophys. J.* **275**, 571 (1983).
- ³P. C. van der Kruit, *Astron. Astrophys. J.* **29**, 231 (1973).
- ⁴J. S. Gallagher, J. W. Goad, and J. Mould, *Astrophys. J.* **263**, 101 (1982).
- ⁵R. W. O'Connell, *Astrophys. J.* **267**, 80 (1983).
- ⁶J. -L. Nieto and M. Auriere, *Astron. Astrophys.* **108**, 334 (1982).
- ⁷A. Sandage and H. L. Johnson, *Astrophys. J.* **191**, 63 (1974).
- ⁸V. M. Lyutyi, *Sov. Sci. Rev. E: Astrophys. Space Phys. Rev.* **1**, 61 (1981)].
- ⁹V. M. Lyutyi, *Astron. Zh.* **54**, 1153 (1977) [*Sov. Astron.* **21**, 655 (1978)].
- ¹⁰A. Lawrence, *Mon. Not. R. Astron. Soc.* **192**, 83 (1980).
- ¹¹T. F. Adams and D. W. Weedman, *Astrophys. J.* **199**, 19 (1975).
- ¹²A. Lawrence, M. G. Watson, K. A. Pounds, and M. Elvis, *Mon. Not. R. Astron. Soc.* **217**, 685 (1985).
- ¹³R. M. Humphreys, *Astrophys. J.* **241**, 587 (1980).
- ¹⁴A. Sandage and G. Carlson, *Astrophys. J.* **267**, L25 (1983).
- ¹⁵M. F. Walker, *Astron. J.* **69**, 744 (1964).
- ¹⁶M. V. Penston, *Mon. Not. R. Astron. Soc.* **162**, 359 (1973).
- ¹⁷E. A. Dibai and V. M. Lyutyi, *Astron. Zh.* **61**, 10 (1984) [*Sov. Astron.* **28**, 7 (1984)].
- ¹⁸D. E. Kleinmann and F. J. Low, *Astrophys. J.* **159**, L165 (1970).

The beam pattern of 1400-MHz double sources

V. R. Amirkhanyan

Shternberg Astronomical Institute, Moscow

(Submitted April 24, 1985; revised September 4, 1985)

Pis'ma Astron. Zh. **12**, 194-197 (March 1986)

Analysis of the statistical distribution of the flux ratios for the components of double radio sources indicates that the angular beam pattern has not only an underlying spherical part but a main lobe about 30° wide aligned with the radio-source major axis.

Mounting evidence indicates that the components of double radio sources radiate isotropically only to a first approximation. Regular magnetic fields are present in these sources,^{1,2} ensuring a complex beaming pattern. It is vital to consider this matter, because the shape of the radio beam will significantly affect the source statistics and thus tie in closely with cosmology. The influence has not yet been assessed, however, since beam shapes have not hitherto been established on the basis of experimental data.

I have sought to fill the gap by making two assumptions:

1. The beam pattern of a double radio source comprises two identical beams oriented in opposite directions, as sketched in Fig. 1.
2. Both beams are axisymmetric about the radio-source major axis.

Then each beam component can be described by a function $A(\theta)$ of a single variable θ , the angle between the line of sight and the major axis.

In view of the assumed symmetry, the observer

will record for the two components a flux ratio

$$\frac{A(\theta - \pi)}{A(\theta)} = f(\theta). \quad (1)$$

Clearly f will depend on the orientation of the radio source relative to the observer, that is, on the angle

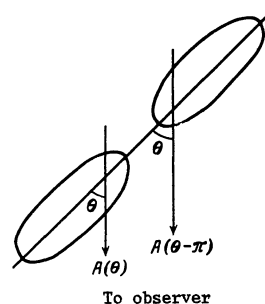


FIG. 1. An idealized model beam pattern for a double radio source.

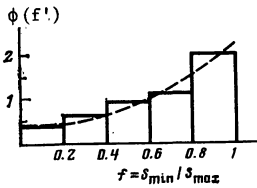


FIG. 2. Distribution function for the component flux ratio f . Dashed curve, a fit $\phi(f) = 0.3 \exp(2.06f)$ to the experimental data.

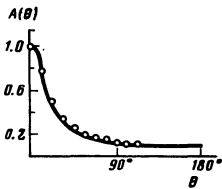


FIG. 3. A control calculation in which an initial beam function $A(\theta)$ with parameter $k = 8$ (circles) is successfully recovered (curve).

6. If we know the relation $f(\theta)$ we can use Eq. (1) to find the unknown beam shape $A(\theta)$.

Let us then proceed to determine $f(\theta)$. Suppose that we are observing an ensemble of double radio sources with identical beams satisfying the assumptions above. If the sources are oriented at random in space, f may take any value from $f_{\min} = A(\pi)/A(0)$ to 1. The f - and θ -distributions are uniquely related to each other, enabling us to establish $f(\theta)$:

$$\int_{f_{\min}}^f \varphi(x) dx = \int_0^\theta \psi(y) dy. \quad (2)$$

In light of the random spatial orientation we will have

$$\psi(\theta) d\theta = \sin \theta d\theta. \quad (3)$$

A distribution function (f) has been derived from experimental surveys^{3,4} of the structure of 1400-MHz sources in the revised Third Cambridge catalog and from surveys at Westerbork⁵ at this same frequency. An important feature has been noticed in the Westerbork survey: the distribution (f) is independent of the flux density for sources throughout the 0.6 mJy–3.5 Jy range, perhaps implying that over wide luminosity and cosmological-distance intervals the beam pattern undergoes little change. Table I and Fig. 2 indicate the resulting distribution of f .

Specifying the distribution analytically as

$$\varphi(f) df = C e^{\alpha f} df$$

and recognizing that

$$N_i/N_2 = \int_{f_{i-1}}^{f_i} \varphi(x) dx,$$

we obtain

$$\varphi(f) df = 0.3 e^{2.06f} df. \quad (4)$$

TABLE I. Paired-Component Flux-Ratio Distribution

$f = S_{\min}/S_{\max}$	N_i	N_i/N_2
0–0.2	14	0.069
0.2–0.4	25	0.123
0.4–0.6	37	0.182
0.6–0.8	45	0.222
0.8–1.0	82	0.404
	$N_2=203$	

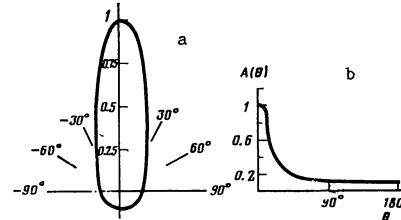


FIG. 4. One component of a double radio-source beam, in: a) polar coordinates; b) rectangular coordinates.

We now substitute the expressions (3), (4) into Eq. (2), perform the integration, and express f in terms of θ :

$$f(\theta) = 1 + \ln [1 - (1 - e^{\alpha(f_{\min}-1)}) \cos \theta] / \alpha. \quad (5)$$

That is all we need to solve Eq. (1).

In arriving at a solution algorithm we have made use of the circumstance that by the displacement theorem the spectra $\ln A(\theta)$, $\ln A(\theta - \pi)$ will differ by the factor $\exp(j\Omega\pi)$. Control calculations have been done to check out the algorithm, a beam shape

$$A(\theta) = 0.1 + 1/(1 + k\theta^2)$$

being specified. Writing the corresponding expression (1) for $f(\theta)$ and solving the inverse problem, one can recover $A(\theta)$; and as Fig. 3 demonstrates, the reconstructed beam is virtually identical with the original beam.

Before proceeding to substitute the distribution (5) into Eq. (1) and calculating the beam of a real radio source, we must decide what the value of f_{\min} is. To judge from the sample at hand, the smallest ratios f_{\min} range from 0.05 to 0.1; only 2 of the 203 objects come within this interval. To assess the influence of the parameter f_{\min} on the final result we have carried out calculations for both $f_{\min} = 0.05$ and $f_{\min} = 0.1$. Figure 4 outlines the radio beam obtained for one component of a double source when $f_{\min} = 0.1$. A main lobe $\pm 17^\circ$ wide stands on a pedestal of ≈ 0.1 amplitude, nearly spherical in shape. Presumably this spherical part represents the emission of relativistic electrons moving in the tangled magnetic fields of the radio-source "ear," while the main-lobe radiation would correspond to a stream of electrons injected by the central body into the regular magnetic field joining the two radio components. If we were to take $f_{\min} = 0.05$ the beam would retain its shape; the pedestal would be ≈ 0.05 high and the main lobe $\pm 13^\circ$ wide.

When calculating spectral-index distributions in a recent paper,⁶ the author estimated at what angles the observer could receive radiation from electrons in a regular magnetic field. It was found that the line

of sight should be inclined to the field direction by at most 14° . This value is about the same as the widths computed above for the main lobe, lending confidence to the belief that we have drawn a fairly realistic picture.

In closing, we would again emphasize that the existence of complex beam patterns should affect the observed flux-density and angular-size distributions of radio sources, and ought to be taken into account in cosmological contexts.

- ¹V. N. Kuril'chik, *Astron. Zh.* **55**, 286 (1978) [*Sov. Astron.* **22**, 169 (1978)].
²Yu. A. Kovalev and V. P. Mikhailutsa, *Astron. Zh.* **57**, 696 (1980) [*Sov. Astron.* **24**, 400 (1981)].
³G. H. Macdonald, S. Kenderdine, and A. C. Neville, *Mon. Not. R. Astron. Soc.* **138**, 259 (1968).
⁴C. D. Mackay, *Mon. Not. R. Astron. Soc.* **145**, 31 (1969).
⁵R. A. Windhorst, G. M. van Heerde, and P. Katgert, *Astron. Astrophys. Suppl.* **58**, 1 (1984).
⁶V. R. Amirkhanyan, *Astrophys. Space Sci.* **108**, 125 (1985).

Has the Crab a radio shell?

S. A. Trushkin

Special Astrophysical Observatory, USSR Academy of Sciences, Nizhniĭ Arkhyz

(Submitted June 25, 1985)

Pis'ma Astron. Zh. **12**, 198-204 (March 1986)

Comparison of $\lambda = 1.38, 2.08$ cm RATAN-600 observations against Velusamy's 20-cm VLA map indicates that the spectral index α holds constant along drift scans across the entire Crab Nebula source. Measurements of wide dynamic range with the high-sensitivity $\lambda = 7.6$ cm RATAN-600 radiometer place a new upper limit on the surface brightness of any circumnebular shell: $\Sigma_{\text{sh}} < 10^{-22}$ on the surface brightness $W^{-2} \text{sr}^{-1} \text{Hz}^{-1}$ on $14'-60'$ scales, contravening the existence of a radio shell around the Crab.

1. INTRODUCTION

The problem of whether the Crab Nebula is surrounded by a shell structure ties in closely with the important question of how to classify the supernova outburst that occurred in 1054. Possibly the Crab may have resulted from a rare type of helium-star explosion in which the nebular remnant expands at low velocity (see, for example, Nomoto¹). In an alternative scenario proposed by Chevalier,² the event of 1054 would have been a normal type II supernova, the rapidly moving envelope of the shattered star not yet having been discovered. Wilson³ has recently discussed the two candidate models.

Although many attempts have been made to detect a shell around the Crab at radio wavelengths (Refs. 4-7), all the findings have thus far been negative. In some of these experiments^{4,5} a structure resembling the remnant of the 1006 supernova would have been observable, but despite more than enough radio sensitivity, no such envelope was found. Nor have recent x-ray observations of the Crab^{6,9} furnished any definitive evidence of a shell. It is only in the optical range that Murdin and Clark¹⁰ were able to discern a sizable envelope extending at least $14'$ along its major axis and $6'$ along the minor

axis from the center of the Crab Nebula. On the basis of comprehensive spectroscopy Clark et al.¹¹ advocate a model in which an inner shell of bright filaments would be linked to an extended halo through an outer shell of fainter but faster-expanding filaments.

This letter presents the results of centimeter-wavelength observations of the Crab, carried out from 1980 to 1984 with the RATAN-600 radio telescope in the Caucasus.

2. OBSERVATIONS

The RATAN-600 north sector was equipped with the regular set of $\lambda = 1.38-31.2$ cm radiometers¹² and operated in the drift regime, with the source transiting the stationary antenna beam. The 7.6-cm radiometer, the most sensitive one, was cooled by a closed-cycle cryogenic system.¹³ Table I gives the radiometer noise thresholds and three basic parameters measuring the beam at each wavelength: the last, $\phi_{0.5}^e$, represents the angular size of the beam envelope as set by the vertical dimension of the elements comprising the main reflector of the radio telescope, while the orthogonal halfwidths $\phi_{0.5}^h, \phi_{0.5}^v$ have been computed from Korzhavin's programs.¹⁴

TABLE I. Radiometer and Beam Parameters

Parameter	λ , cm						
	1.38	2.08	3.9	7.6	8.2	13.0	31.2
T_n , mK	60	50	13	3	9	30	60
$\phi_{0.5}^h$, $1''$	13	19	26	56	61	96	230
$\phi_{0.5}^v$, $1'$	1	1.4	2.7	5.8	6.2	9.9	24
$\phi_{0.5}^e$, $1'$	8.5	13	22	44	47	75	180